Determination of Intergranular Strain State in a β-Ti alloy with Rod Texture

T.M. Holden[1*] , **J.W.L. Pang**[2], and **R.L. Donaberger** [3]
[1] Northern Stress Technologies, 5 Spring Rd., Deep River, Ontario, Canada K0J 1P0
[2] Materials Science & Technology Division, Oak Ridge National Laboratory, Oak Ridge, Tennessee 37831, USA
[3] National Research Council, Steacie Institute for Molecular Sciences, Chalk River, Ontario K0J 1J0, Canada

The manuscript was received on 12 November 2008 and was accepted after revision for publication on 23 January 2009.

DOI:10.1243/03093246JSA378

Abstract: In this experiment, the intergranular strains in the centre of a β-Ti rod generated during the manufacturing processes were measured. The intergranular strains reflect the nature of the plastic deformations undergone in manufacture. Qualitative descriptions of the plastic history have been made from the measurements at present. The results demonstrated the possibility of assessing the level of inhomogeneous plastic deformation.

Keywords: titanium alloy, intergranular strain

1 INTRODUCTION

Residual stresses are generated in a material whenever it is plastically deformed in an inhomogeneous manner. On a macroscopic scale, this leads to type-1 stresses and on the size scale of the grains to intergranular or type-II stresses (1,2). Plastic deformation takes place preferentially in particular slip or twinning systems. Thus, the degree of plastic deformation of each grain within a polycrystal is sensitive to its orientation with respect to the applied forces. The differences in the deformation of grains of different orientations are compensated by intergranular stresses within the individual grains. These stresses are balanced over a small volume element of the material containing a sufficiently large number of grains. The type-I stresses must balance over a section of the component.

In recent years, intergranular strains have attracted much interest. Measurements of intergranular strain generated by uniaxial applied stresses have been carried out with many face-centred cubic (3-5) and hexagonal alloys (6). Measurements reported on body-centred cubic materials have been limited to ferritic steel with mild rolling texture to date (7). In this paper, measurements of intergranular strains in a bcc β-Ti drawn rod in its 'as-received' condition are described. The determination of the intergranular strain state of the grains was made possible by the presence of the fibre texture with dominant $< 110 >$ crystallographic orientation parallel to the rod axis. The experiment shows that the magnitudes of intergranular strains are far from negligible and also indicates the possibility of projecting the plastic deformation history from the intergranular strain state of the specimen.

2 SPECIMENS

The β-Ti alloy rod, which derives its superior mechanical properties from α-precipitates, was provided by *TIMET*. The rod was cold drawn from a 0.598" coil in turn made by hot rolling a forged 3.625" billet. The rod has been solution heat treated and ground to a finished size of 0.530" in diameter. The chemical composition of the alloy is $Ti_{87.0}Mo_{6.7}Fe_{4.7}Al_{1.4}O_{0.2}$ by weight with trace amounts of Si, Cu, C and N. The yield strength and the bulk Young's Modulus are $\sim$ 957 MPa $\sim$ 92 GPa

Corresponding author: Northern Stress Technologies, 5 Spring Rd., Deep River, Ontario, Canada K0J 1P0. email: holdent@magma.ca

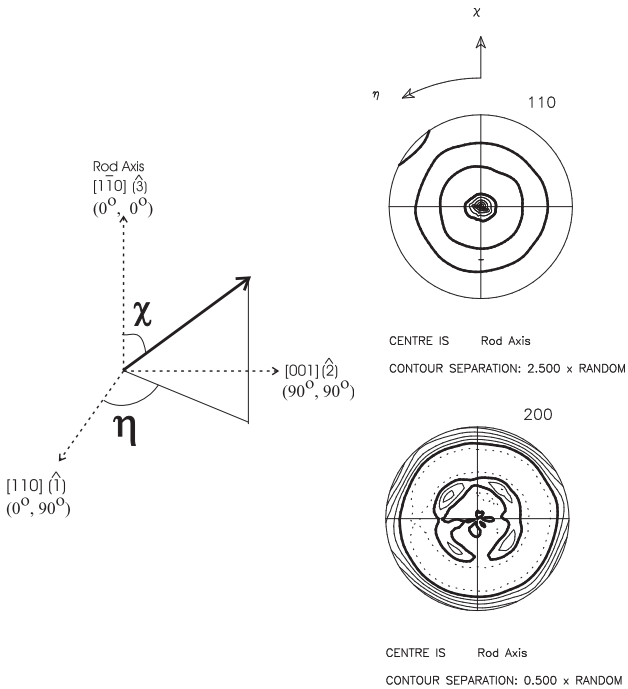

Fig. 1: a) The sample spherical and the crystal coordinate systems for the specimen; b) pole figure for the (110) reflection; and c) pole figure for the (200) reflection. Heavy solid lines are the random contours. Contours above random are indicated by solid lines, and dotted lines represented contours below random.

respectively.

Two coupons of 0.16" in diameter were cut out from the centre of the rod to optimise the diffracted neutron intensity since the coherent cross section is small and the incoherent and absorption cross sections are relatively high as discussed later. The cutting process would tend to remove any macroscopic stresses in the coupon. One of the coupons was heated to 720°C for 5 minutes and then air cooled. This annealing procedure was carried out to remove the stresses remaining in the coupon. The specimens with and without annealing were labelled as S_{as-is} and $S_{annealed}$ respectively.

3 EXPERIMENTAL PROCEDURE

The experiment was carried out on the E3 spectrometer of the Steacie Institute for Molecular Sciences at Chalk River, Canada. The lattice spacings d_{hkl} of sets of planes with normal vector $[hkl]$ parallel to the scattering vector are determined by measuring the diffracted angle $2\theta_{hkl}$ and using Bragg's law. The strains were calculated with

Table 1: Reflections and the corresponding angular positions at which measurements were made.

(hkl)	(η, χ)	(hkl)	(η, χ)
$(1\bar{1}0)$	$(0°, 0°)$	$(1\bar{3}0)$	$(54.44°, 26.5°)$
(301)	$(0°, 47.9°)$	(200)	$(54.44°, 45°)$
(110)	$(0°, 90°)$	$(1\bar{1}2)$	$(54.44°, 54.73°)$
$(2\bar{1}1)$	$(90°, 30°)$	(112)	$(54.44°, 90°)$
$(\bar{1}12)$	$(90°, 64.76°)$		
$(0\bar{1}3)$	$(90°, 71.3°)$		
(002)	$(90°, 90°)$		

$$\epsilon_{hkl} = \frac{d_{hkl} - d^0_{hkl}}{d^0_{hkl}}, \qquad (1)$$

where d^0_{hkl} is the stress-free lattice spacing. Descriptions of the techniques of neutron diffraction strain measurements can be found in the literature (8-10).

The texture of the S_{as-is} sample was determined by measuring the diffracted neutron intensity of (110), (200) and (111) reflections on a 5° grid over the spherical coordinates (η, χ) shown in Figure 1a where χ is the angular deviation from the rod axis and η is the azimuthal angle. The pole figures for the (110) and (200) reflections are shown in Figure 1b and c. Near cylindrical symmetry of the bcc fibre texture was observed and (110) reflections had intensities more than 15 times above random along the rod axis. The departures from cylindrical symmetry for the (200) poles in the ring of intensities at $\chi \sim 35°$ suggests that the rolling texture generated during hot rolling has not been fully erased by the cold drawing process. A crystal coordinate system to describe the orientation of the grains with respect to the rod axis is also shown in Figure 1a. The $< 1\bar{1}0 >$ crystal axis is parallel to the rod axis ($\hat{3}$). Since the texture transverse to the rod axis is almost random and axes, the axes $\hat{1}$ and $\hat{2}$ are evenly distributed in the transverse plane. Taking advantage of the strong rod texture, a single strain tensor for the grains, since they are highly aligned, was determined by making measurements with the appropriate reflections at the specific angular positions (η, χ) listed in Table 1.

A neutron wavelength of 1.5127Å, diffracted from a (115) reflection of a squeezed Ge monochromator, was used. The collimation of the neutron beam before and after diffraction of the sample was 0.4°. The sample was fully bathed in the neutron beam to ensure the macroscopic strain components, if they exist, are averaged out to zero. The reference parameter, which appears to be unaffected by intergranular stresses, was determined by making the same measurements with $S_{annealed}$ at the same angular coordinates as for S_{as-is}.

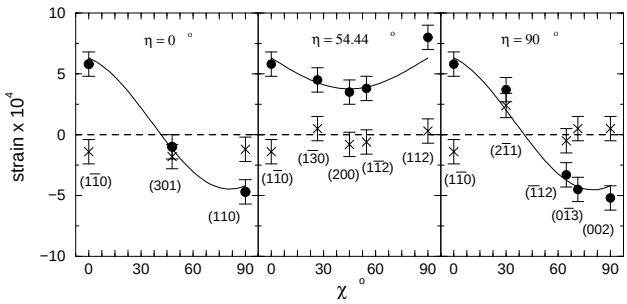

Fig. 2: Residual strains of the S_{as-is} and the $S_{annealed}$ samples, represented by solid circles and crosses respectively. The solid lines are the calculated strains from the fitted strain tensor for the S_{as-is} sample. The reflection for each measurement is shown by the side of each data point. Measurements were made as a function of χ at $\eta = 0°$, $54.44°$ and $90°$.

4 RESULTS

The reference parameter a^0 determined by averaging all the measurements for $S_{annealed}$ is 3.2443 ± 0.0002Å. The corresponding strains for $S_{annealed}$ are shown in Figure 2 and are found to be zero within errors so that the annealed state is stress free. The strain measurements for S_{as-is} are shown in the same figure. The experimental errors are similar to the annealed sample. Tensile strains are found along $\eta = 54.44°$ with largest magnitude of $8.0 \pm 1.3 \times 10^{-4}$ at $(54.44°, 90°)$. Compressive strains are found at angular positions between the rod axis $< 1\bar{1}0 >$ and the other two principal axes $< 110 >$ and $< 002 >$ in the transverse planes.

The average lattice parameter for S_{as-is} is 3.2446 ± 0.0003Å which agrees with the a^0 determined with $S_{annealed}$ within errors. This provides an important cross-check for the stress-free lattice parameter. If the chemistry of the alloy had been altered by the annealing process, the stress-free lattice parameters of the two samples would be different.

The strain tensor of the grains in the specimen S_{as-is} was resolved based on the measurements and the values of the components are given in Table 2. Strain at angular position (η, χ) can be expressed in terms of the strain tensor components as follows:

$$\begin{aligned}\epsilon_{\eta\chi} = {} & \epsilon_{11}\cos^2\eta\sin^2\chi + \epsilon_{12}\sin2\eta\sin^2\chi + \\ & \epsilon_{22}\sin^2\eta\sin^2\chi + \epsilon_{33}\cos^2\chi + \\ & \epsilon_{13}\cos\eta\sin2\chi + \epsilon_{23}\sin\eta\sin2\chi. \end{aligned} \quad (2)$$

The strain at $\eta = 0°, 54.44°$ and $90°$ of the S_{as-is} sample were calculated with Equation as a function of χ. The calculated values are shown in Figure 2 together with the measurements. Good agreement between measurements and calculations was observed.

Table 2: Components of the strain tensor of the grains of S_{as-is}. All values are in the units of 10^{-4}.

ϵ_{11}	ϵ_{22}	ϵ_{33}
-4.2 ± 0.7	-4.2 ± 0.8	6.3 ± 0.7
ϵ_{23}	ϵ_{13}	ϵ_{12}
-1.9 ± 1.2	-1.7 ± 1.4	11.1 ± 1.6

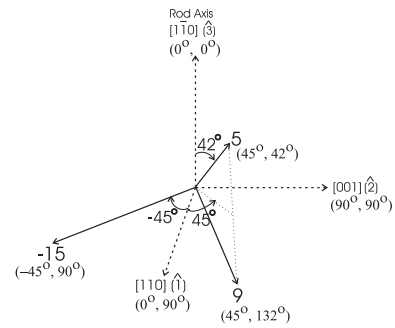

Fig. 3: The principal directions of the residual strain tensor of the S_{as-is} sample with respect to the crystal coordinate system of the grains of the sample. The magnitudes of the strain components are indicated by the principal directions and are all in the units of 10^{-4}.

5 DISCUSSION

The principal directions and the corresponding magnitudes of the strain tensor are illustrated schematically in Figure 3. The sum of the principal components is $-2 \pm 3 \times 10^{-4}$ which is zero within errors. This is not unexpected as intergranular strains are generated by deformation misfits between crystallographic directions and must be balanced over a texture weighted summation of all grain orientations. Since the strain state measured applies to almost all the grains in the specimen, the first invariant of the strain tensor is equivalent to the summation of strains of all the grains.

Another interesting observation is that all the principal directions of the strain tensor are far from parallel to the sample axes. This suggests that the applied forces causing inhomogeneous plastic deformation were not uniaxial along obvious geometric sample directions but were multiaxial with a large shearing component. This conclusion is in accordance with the deformation history of the specimen which has been subjected to rolling and drawing. In these processes, large compressive pressures would have been applied by the die in the transverse planes

of the rod in addition to the drawing force along the axis. Large shearing forces due to friction between the die and the material would have occurred (11).

The corresponding stresses could be calculated if the elastic constants, C_{ij}, of β-Ti were known. However, these quantities have not been determined experimentally and it was beyond the scope of this experiment to make measurements of the diffraction elastic constants. The principal stresses were instead expressed in terms of C_{ij}. For a cubic material, the elastic constants C_{ij} are referred to the coordinate system, L, with axes ($< 100 >, < 010 >, < 001 >$). In order to calculate the stresses in, L$'$, with axes parallel to the eigenvectors of the strain tensor, the elastic constants were transformed from L to L$'$. The transformed elastic constants C'_{ij}, are shown in Table 3. The principal stresses, σ_i, were determined by $\sigma_i = C'_{ij}\epsilon_j$ and the values are given in Table 4. The sum of the components of $\{\sigma_i\}$ is $2C_{12}$ - C_{11} which means that stress balance for the single stress tensor is fulfilled if $\frac{C_{11}}{C_{12}} = 2$. In comparison to the elastic constants of other bcc elements such as V and Fe whose $\frac{C_{11}}{C_{12}}$ ratios are 1.95 and 1.72 respectively (12), it is likely that the same ratio for β-Ti is of the order of 2. The stress component along the rod axis, σ^A, was resolved to be $2C_{11}$ - $3.25C_{12}$ -$10C_{44}$, using the stress tensor shown in Table 4. The lack of the magnitudes of the elastic constants of β-Ti has prevented a cross-check for stress balance in the longitudinal direction of the specimen.

We note however that the strain in the axial direction is relatively large, $5.8 \pm 1.0 \times 10^{-4}$, and it would be somewhat fortuitous if the corresponding axial stress was zero. Recall, however, that the sample was cut from the centre of the rod. A texture gradient is anticipated along the radius of the rod, since the plastic deformation from surface to centre would be expected to vary. In addition, intergranular stresses would also be expected to vary with radial position. It is reasonable, therefore, that there should be a variation of axial stress with radial position which would balance over the radius of the rod. Also, the intergranular effects which have been observed may be partly balanced by the stresses in the α-precipitates which give the alloy its superior mechanical properties. We have not measured the stress tensor in the α-phase, and this may be difficult to do since the concentration is low and therefore the diffraction intensity will be weak.

It is interesting to note that it would have been impossible to make measurements on β-Ti if the material had not been so strongly textured. The coherent scattering cross-section is only 1.78×10^{-24} cm^2 on account of the alloying elements, conversely the incoherent cross-section is 2.67×10^{-24} cm^2, and the absorption cross-section is 5.77×10^{-24} cm^2. This implies that the intrinsic background from the sample under the diffraction peaks would be greater than the peak intensity if there is no crystallographic texture.

Table 3: The non-zero elastic constants refer to the coordinate system with principal axes parallel to the eigenvectors of the strain tensor. C_{11}, C_{22} and C_{44} are the elastic constants in the crystal coordinate system with principal directions ($< 100 >, < 010 >, < 001 >$), and it has been assumed that the principal directions are 45° from the geometrical axes.

$$
\begin{aligned}
&C'_{11}=C'_{22}=\tfrac{1}{2}C_{11}+\tfrac{1}{2}C_{12}+C_{44},\\
&C'_{33}=C_{11},\\
&C'_{12}=C'_{21}=\tfrac{1}{2}C_{11}+\tfrac{1}{2}C_{12}-C_{44},\\
&C'_{13}=C'_{31}=C'_{23}=C'_{32}=\tfrac{3}{2}C_{12},\\
&C'_{44}=C'_{55}=C_{44},\\
&C'_{66}=\tfrac{1}{2}C_{11}-\tfrac{1}{2}C_{12}.
\end{aligned}
$$

Table 4: The principal directions and the corresponding components of the stress tensor of the grains of S_{as-is}. All values are expressed in terms of C_{11}, C_{12} and C_{44}.

Principal Dirs (η, χ)	Stress
$(45°, 132°)$	-$5C_{11}$ + $8.5C_{12}$ - $20C_{44}$
$(-45°, 90°)$	-$5C_{11}$ + $8.5C_{12}$ + $20C_{44}$
$(45°, 42°)$	$9C_{11}$ - $15C_{12}$

Although only qualitative descriptions of the plastic history can be made from the measurements at present, the results demonstrated the possibility of assessing the level of inhomogeneous plastic deformation. Further systematic studies on specimens with different levels of deformation may allow quantitative assessment of the deformation history which will also be invaluable for the development of finite element and self-consistent modelling of deformation on the microscopic level.

ACKNOWLEDGEMENTS

The authors would like to thank Dr. Paul Allen of Timet and Tom King of Rockwell International, Toronto for providing the materials and their manufacturing specifications. We wish to thank Wayne Ferris of Atomic Energy of Canada Limited for carrying out the heat treatment. We would also like to express our gratitude to J.H. Fox and L.E. MacEwen for experimental assistance. Research at ORNL is supported by DoE BES Division of Materials Sciences under contract with UT-Battelle, LLC.

REFERENCES

1 **Hosford, W.F.** The Mechanics of Crystals and Textured Polycrystals. New York: Oxford University Press, 1993.

2 **Noyan, I.C.** and **Cohen, J.B.** Residual Stress Measurement by Diffraction and Interpretation. New York: Springer-Verlag, 1987.

3 **Clausen, B., Lorentzen, T.,** and **Leffers, T.** Acta. Metall. 1998;46:3087.

4 **Pang, J.W.L., Holden, T.M.,** and **Mason, T.E.** Acta mater. 1998;46:1503.

5 **Holden, T.M., Clarke, A.P.,** and **Holt, R.A.** Metall. Trans. A. 1997;28A:2565.

6 **Pang, J.W.L., Holden, T.M., Turner, P.A.,** and **Mason, T.E.** Acta mater. 1999;47:373.

7 **Pang, J.W.L., Holden, T.M.,** and **Mason, T.E.** J. Strain Analysis. 1999;33:373.

8 **Holden, T.M.** Handbook of Measurement of Residual Stresses, Society for Experimental Mechanics. Liburn, Georgia: The Fairmont Press, 1996: Chapter 6.

9 **Hutchings, M.T.** Measurements of residual and applied strain using neutron diffraction. Dordrecht: Kluwer Academic Publishers, 1992.

10 **Holden, T.M., Root, J.H., Fidleris, V., Holt, R.A.,** and **Roy, G.** Mater. Sci. Forum. 1988;27/28:359.

11 **Dieter, G.E.** Mechanical Metallurgy 3rd edition. New York: McGraw-Hill, 1986.

12 Edited by **Brandes, E.A.,** and **Brook, G.B.** Smithells Metals Reference Book seventh edition. Butterworth Heinemann, 1992.